Chaperone-assisted Excisive Recombination, a Solitary Role for DnaJ (Hsp40) Chaperone in Lysogeny Escape

Stéphanie M Champ, Tania Puvirajesinghe, Elsa M Perrody, Rachid M Menouni, Pierre M Genevaux, Mireille M Ansaldi

THE JOURNAL OF BIOLOGICAL CHEMISTRY VOL. 286, NO. 45, pp. 38876–38885, November 11, 2011

Chaperone-assisted Excisive Recombination, a Solitary Role for DnaJ (Hsp40) Chaperone in Lysogeny Escape*

Received for publication, July 12, 2011, and in revised form, September 9, 2011 Published, JBC Papers in Press, September 9, 2011, DOI 10.1074/jbc.M111.281865

Stéphanie Champ[‡], Tania M. Puvirajesinghe[‡1], Elsa Perrody[§], Rachid Menouni[‡], Pierre Genevaux[§], and Mireille Ansaldi[‡2]

From the [‡]Laboratoire de Chimie Bactérienne CNRS UPR9043, Institut de Microbiologie de la Méditerranée, Aix-Marseille Université, 31 chemin Joseph Aiguier, 13402 Marseille Cedex 20, France and [§]Laboratoire de Microbiologie et Génétique Moléculaires CNRS UMR 5100, Université Paul Sabatier, 118 route de Narbonne, 31062 Toulouse Cedex 9, France

Background: Site-specific recombination is involved in the temperate phage lysogeny cycle.
Results: DnaJ is recruited by a protein specific for excisive recombination.
Conclusion: *Bona fide* chaperone activity of DnaJ enhances prophage excision.
Significance: Stress response in *E. coli* contributes to mobilization of temperate phages.

Temperate bacteriophage lytic development is intrinsically related to the stress response in particular at the DNA replication and virion maturation steps. Alternatively, temperate phages become lysogenic and integrate their genome into the host chromosome. Under stressful conditions, the prophage resumes a lytic development program, and the phage DNA is excised before being replicated. The KplE1 defective prophage of *Escherichia coli* K12 constitutes a model system because it is fully competent for integrative as well as excisive recombination and presents an atypical recombination module, which is conserved in various phage genomes. In this work, we identified the host-encoded stress-responsive molecular chaperone DnaJ (Hsp40) as an active participant in KplE1 prophage excision. We first show that the recombination directionality factor TorI of KplE1 specifically interacts with DnaJ. In addition, we found that DnaJ dramatically enhances both TorI binding to its DNA target and excisive recombination *in vitro*. Remarkably, such stimulatory effect by DnaJ was performed independently of its DnaK chaperone partner and did not require a functional DnaJ J-domain. Taken together, our results underline a novel and unsuspected functional interaction between the generic host stress-regulated chaperone and temperate bacteriophage lysogenic development.

Temperate phages have great importance in mediating gene transfer and inactivation in bacteria. Prophage genes can confer selective advantage through a superinfection mechanism and often increase the pathogenic properties of some strains for example through the acquisition of toxin genes (1). In the lysogenic state, prophages occasionally lose genes involved in productive growth in which case the strain is no longer able to liberate infectious particles. Such prophages are termed defective, but nevertheless, they can inactivate host genes or conserve genes important for host pathogenicity or fitness (2).

Phage λ has long served as a model system for studies of regulated site-specific recombination (3). Indeed, temperate bacteriophages, such as λ, may choose between lytic and lysogenic cycles for their propagation in the bacterial host (for a review, see Ref. 4). Under favorable conditions for bacterial growth, the phage genome is inserted into the host genome by an integrative recombination reaction, which takes place between DNA attachment sites called *att*P and *att*B in the phage and bacterial genomes, respectively. As a result, the integrated prophage DNA is bound by hybrid attachment sites termed *att*L and *att*R. In response to changes in the physiological state of the bacteria, mainly in response to stress conditions, such as DNA damage, phage DNA is excised from the host chromosome. This excisive reaction allows *att*L and *att*R to recombine and restores the *att*P and *att*B sites on the circular phage and host genomes. Although the phage-encoded integrase (Int)[3] protein catalyzes both integrative and excisive reactions, it requires the assistance of several accessory proteins depending on the direction of the reaction. The host-encoded integration host factor (IHF) is required for both integration and excision, whereas the phage-encoded excisionase (Xis) is necessary for excision only and prevents reintegration (5, 6). Excisionase binds and bends DNA, assists the formation of the intasome, and controls the directionality of the reaction toward excision; therefore, these proteins were also named recombination directionality factors (RDFs) (7). Moreover, directionality of the excisive reaction is conferred by the irreversibility of multiple reaction steps (8).

The KplE1 prophage (also named CPS-53) is one of the 10 prophage regions present in *Escherichia coli* K12 MG1655 (9). It is a defective prophage integrated into the *argW* tRNA gene, and the remaining genome (10.2 kb) of the prophage contains 16 open reading frames (ORFs) bordered by a duplicated core sequence of 16 nucleotides (CTGCAGGGGACACCAT).

* This work was supported by CNRS, the French Research Ministry (*Ministère de l'Education Nationale de la Recherche et de la Technologie*), and National Research Agency Grant ANR-08-BLAN-0122-01 (to M. A. and P. G.).
[1] Present address: Polarité cellulaire signalisation et cancer, Centre de Recherche en Cancérologie de Marseille, INSERM UMR 891, 27 Blvd. Leï Roure, BP 30059, 13273 Marseille Cedex 09, France.
[2] To whom correspondence should be addressed. Tel.: 33-4-91-16-45-85; Fax: 33-4-91-71-89-14; E-mail: ansaldi@ifr88.cnrs-mrs.fr.

[3] The abbreviations used are: Int, integrase; Hsp, heat shock protein; IHF, integration host factor; RDF, recombination directionality factor; SSR, site-specific recombination; Q-PCR, quantitative PCR; Xis, excisionase; Tricine, *N*-[2-hydroxy-1,1-bis(hydroxymethyl)ethyl]glycine.

Despite the small remnant genome, the KplE1 prophage can be excised *in vivo* (10, 11). Analysis of the KplE1 recombination module has shown that the prophage contains all the elements required for site-specific recombination to occur, including RDF and integrase genes as well as the *att*L and *att*R recombination regions (12). This recombination module is highly conserved in several enterobacteria phage genomes, such as HK620 and Sf6 that infect *E. coli* strain TD2158 and *Shigella flexneri*, respectively (13, 14). *In vivo* recombination studies are made easier by the defective nature of the KplE1 prophage; indeed, the excisive recombination and its regulation can be dissected *in vivo* independently of prophage induction.

The *torI* gene is the last gene of the KplE1 prophage genome and was originally identified using a genetic multicopy approach as a negative regulator of the *torCAD* operon that encodes the trimethylamine-oxide reductase respiratory system in *E. coli* (15). Despite its role as an inhibitor of the TorR response regulator, later work has shown that TorI is in fact a *bona fide* RDF for KplE1 phage excision (10). TorI shares several properties with other RDFs, such as a small size and a basic pI, and despite no primary sequence homology, its solution structure is highly similar to that of well characterized excisionases, such as $^{\lambda}$Xis and ^{Tn916}Xis (16, 17). *In vitro*, TorI controls directionality of KplE1 site-specific recombination mediated by the IntS tyrosine recombinase (12), and its expression in *E. coli* rapidly leads to the complete excision of KplE1 prophage from the host chromosome (10). Indeed, IntS is permanently expressed in *E. coli* cells at a sufficient level to allow excisive recombination as soon as the TorI RDF is produced, meaning that *in vivo* excision of KplE1 relies on RDF gene expression (18).

Molecular chaperones form a large family of cellular machines, which facilitate protein folding mainly by protecting non-native proteins from misfolding and aggregation (19). They generally act through cycles of binding and release of hydrophobic polypeptide segments that are often buried in the native form of proteins. Alternatively, chaperone "clients" can be found in native complexes, and in this case, molecular chaperones orchestrate specific remodeling, leading to various cellular activities (20). As the successful proliferation of phages requires a substantial reprogramming of the biosynthetic machinery of the host cell and the subsequent folding of a large number of the phage-encoded proteins necessary for viral replication and virion assembly, it is thus not surprising that host- and/or phage-encoded molecular chaperones are central to several key stages of the viral life cycle (21). Remarkably, both major molecular chaperone families, *i.e.* DnaK (Hsp70) and GroEL (Hsp60), were originally discovered as essential host factors for phage development (22–26). The crucial role played by the stress-regulated multifunctional DnaK/DnaJ/GrpE chaperone machine (27) during initiation of phage λ replication well illustrates the involvement of molecular chaperones in temperate phage development. Indeed, DnaK, assisted by its cochaperones DnaJ and GrpE, orchestrates several key steps, leading to the activation of the DnaB helicase in the preprimosomal complex and the subsequent initiation of λ replication (28). In this case, (i) the DnaJ cochaperone first binds to λP and DnaB proteins at the preprimosome and stabilizes the complex. (ii) DnaJ binding facilitates the recruitment of its DnaK chaperone partner to the complex and stimulates the interaction of DnaK with λP. (iii) The formation of a stable DnaK-λP complex induces the dissociation of λP from DnaB, thus initiating DNA replication. (iv) DnaK is then recycled with the help of its GrpE cochaperone, which accelerates nucleotide exchange and indirectly λP release (29).

In this work, we present a novel role for host-encoded molecular chaperones during early stages of phage development. Indeed, we have isolated the DnaJ chaperone as a major protein partner of the TorI RDF and demonstrated that such interaction was critical for the excision process to occur both *in vivo* and *in vitro*. Remarkably, stimulation by DnaJ did not require its DnaK chaperone partner. Our discovery that DnaJ may act as a solitary chaperone assisting TorI excisionase during KplE1 prophage excision sheds light on different levels of regulation of the temperate phage life cycle by molecular chaperones from the heat shock response.

EXPERIMENTAL PROCEDURES

Bacterial Strains, Plasmids, and Media—Bacterial strains and plasmids are listed in Table 1. Strains were grown in LB medium supplemented when necessary with ampicillin (50 $\mu g \cdot ml^{-1}$), chloramphenicol (25 $\mu g \cdot ml^{-1}$), kanamycin (25 $\mu g \cdot ml^{-1}$), L-arabinose (0.2%, w/v), or isopropyl 1-thio-β-D-galactopyranoside (1 mM).

TorI Magnetic Pulldown—The TorI pulldown assay was performed using carboxyl Adembeads (Ademtech). These beads are 300-nm superparamagnetic nanoparticles presenting a polymer core shell structure and a high density of carboxyl groups (>350 $mol \cdot g^{-1}$). Activation and coating of the beads were performed as follows. 20 μl (0.6 mg) of carboxyl beads were washed twice in activation buffer, resuspended in 500 μl of activation buffer before incubation with 48 μl of *1-ethyl-3-(3-dimethylaminopropyl)carbodiimide* cross-linker (4 $mg \cdot ml^{-1}$) for 10 min at 40 °C under agitation. Purified TorI (15 μl at 5 $mg \cdot ml^{-1}$) in activation buffer was then added before incubating the beads for a further 2 h at 40 °C with shaking (800 rpm in an Eppendorf Thermomixer). Control beads were incubated with 5 $mg \cdot ml^{-1}$ BSA in activation buffer. Saturation was performed by adding 120 μl of 0.5 $mg \cdot ml^{-1}$ BSA in activation buffer. Coated beads were then washed twice and resuspended in 250 μl of storage buffer.

TorI-coated and control beads were then incubated with a soluble fraction of MC4100 cells collected in midexponential growth. The cell culture (100 ml) arrested at an A_{600} of 0.9 was centrifuged for 10 min at 8000 rpm (Eppendorf A-4-44 rotor) and resuspended in 1.5 ml of 40 mM Tris. Cells were lysed with a French press (cell pressure, 14,000 p.s.i.), and cell debris was removed by centrifugation for 20 min at 20,000 rpm (Sorvall SS-34 rotor). The soluble fraction was obtained after ultracentrifugation for 60 min at 45,000 rpm (Beckman 70.1 Ti rotor). Coated beads (150 μl) were incubated with 350 μl of the soluble fraction and incubated for 90 min at 20 °C with shaking (800 rpm). Beads were washed three times in 40 mM Tris buffer, pH 7.4 until no coloration was obtained with Bradford solution. Elution from the beads was performed by addition of 40 μl of denaturing loading buffer and incubation for 5 min at 95 °C.

TABLE 1
Strains, plasmids, and primers

	Genotype/sequence	Description	Source/Ref.
Strains			
MC4100			*M. C. Casadaban*
C600 dnaJ259, Tet^R			*36*
LCB6094	*MC4100 dnaJ*259, Tet^R		*This work*
A137	*MC4100 dnaJ*::Tn*10–42*		*57*
Δ[3]	*MC4100 dnaJ*::Tn*10–42*, Δ*cbpA*::*kan*, Δ*djlA*::*spc*		*57*
Plasmids			
pGPJ-His	Ap^R	*pBAD22 vector containing dnaJ* coding sequence with a His_6 tag	*30*
pJH33Q	Ap^R	*pGPJ-His derivative containing His-33 to Gln mutation*	*30*
pJdelH2-His	Ap^R	*pGPJ-His derivative containing DnaJ helix 2 deletion (residues 18–32)*	*This work*
Primers			
JdelH2dir	***CCGGACCGTAACCAGGGTGACAA***A[a]		
JdelH2	***TTGTCACCCTGGTTACGGTCCGG***CGCTGTTTTGGAAACGCCTA[a]		
pBADup	*TACCTGACGCTTTTTATCGCA*		
pBAD-seq2	*GGGACCACCGCGCTACTGCCGCCAGGC*		
attL-pro	*AATGGATATAACGAGCCCCTCC*		
attL-ter-Cy5	*Cy5-CATCGAGAAGGCGGTATGGTTTTTC*		
pnupG-L-Cy5	*CGCTGACGACCCGCCAT*		
pnupG-R	*AGCCAACTTCCCCACAGACAGAA*		
attL-SpeI	*GACTAGTTTCAATCTGCTTAACGGTGAGCAT*		
attL-KpnI	*GGGGTACCGCTAATTGCAGGTTCGATTCC*		
attR-XbaI	*GCTCTAGAGGTTTTAGGGATAAACACAAGGATG*		
attR-IHF2	*CTCTTAAGCCGCGCCAATGG*		
mglC-L	*ATATTCTCACCCAGTCATCG*		
mglC-R	*TGGCACAGACAATCAGAATA*		
htpG-L	*GAAAGGACAAGAAACTCGTG*		
htpG-R	*AGATGGTCAATCACTTCGTC*		
gpt-L	*ATGAGCGAAAAATACATCGT*		
gpt-R	*TACAAACGGTATCGACATGA*		

[a] Bold sequence indicates overlapping sequences.

Eluted proteins were then separated on a Tris-Tricine-SDS 10% acrylamide gel. Bands only appearing in the presence of TorI and in three independent experiments were identified with MALDI-TOF mass spectrometry.

Mass Spectrometry Analysis—Analysis was performed on a MALDI-TOF Microflex II mass spectrometer (Bruker) at the IFR88 Proteomic facility. Tryptic peptides were acquired in positive reflectron mode. The peptide identification was performed using BioTools with internal calibration on the theoretical tryptic peptides of the proteins of interest. We allowed up to four miscleavages and a mass tolerance of 60 ppm for this tryptic peptide analysis.

Immunoprecipitation—The *E. coli* Δ^3 strain harboring the pGPJ-His plasmid (30) was transformed with pBTorI (15). Cells were grown until A_{600} reached 0.5 unit. Proteins expression was induced with 0.2% L-arabinose. Bacterial cells were lysed by sonication (10 pulses of 15 s) in lysis buffer (50 mM Tris-HCl, pH 8.0, 150 mM NaCl, 1% Nonidet P-40), which contained protease inhibitors (Calbiochem). Cell lysates were then subjected to immunoprecipitation using TorI-specific IgGs and incubated overnight at 4 °C. Superparamagnetic nanoparticles conjugated with protein A (Ademtech) in combination with magnetic separation were used to isolate specific antibody-protein complexes. Following three washes with lysis buffer, specifically bound proteins were eluted from beads using non-reducing sample loading buffer (0.25 M Tris-HCl, pH 6.8, 10% glycerol, 2% SDS, 0.05% (w/v) bromphenol blue). Samples were then separated using 10% SDS-Tricine PAGE and transferred to nitrocellulose membrane (Invitrogen) for Western blotting. Membranes were blocked for 1 h with phosphate-buffered saline (PBS) containing 5% skimmed milk powder. Blots were then incubated overnight with polyclonal rabbit primary antibodies recognizing DnaJ (diluted 1:1000). Blots were washed three times with PBS and then incubated with anti-rabbit HRP-conjugated antibody (1:10,000; Amersham Biosciences) for 1 h at room temperature (RT). After washing three times at RT with PBS, blots were developed with ECL SuperSignal West Pico chemiluminescent substrate (ThermoScientific).

Plasmid Construction/J-domain Mutagenesis—To construct plasmid pJdelH2-His, the sequence corresponding to the J-domain flexible helix 2 (residues 18–32) of DnaJ was deleted by a one-step PCR method (31) using plasmid pGPJ-His as a template and overlapping divergent primers. The sequence accuracy of constructions was checked by colony PCR and sequencing using the pBADup and pBAD-seq2 primers. All primer sequences and plasmids are listed in Table 1.

Protein Purification—IntS, TorI, and IHF proteins were overproduced and purified to homogeneity as described previously (12, 15). All proteins were dialyzed in 40 mM Tris-HCl buffer, pH 7.6 containing 50 mM KCl and 10% glycerol. The protein concentrations were estimated by the Bradford method.

DnaJ wild-type and mutants proteins were overproduced from the Δ^3 strain harboring plasmid pGPJ-His, pJdelH2-His, or pJH33Q. Cells were grown at 30 °C in LB medium with ampicillin until the A_{600} reached 0.5 unit, gene expression was then induced by the addition of 0.2% L-arabinose, and incubation continued for 4 h at 30 °C. Cells were pelleted; resuspended in 50 mM Tris-HCl, pH 7.6, 1 M NaCl, 20 mM imidazole, 20 mM β-mercaptoethanol, 0.5% Triton X-100, 0.6% Brij 58P (buffer A), DNase I, 1× protease inhibitor mixture set (EDTA-free; Calbiochem). Cells were lysed using a French press (cell pressure, 14,000 p.s.i.), and the supernatant was loaded onto a 1-ml nickel column (HisTrap™ FF, GE Healthcare) previously equilibrated with buffer A. The column was washed with 10 column volumes. To avoid precipitation of proteins, the detergents (Triton X-100 and Brij 58P) were gradually removed and compensated by a glycerol step gradient from 0 to 50%. To ensure total detergent removal, the column was washed with buffer B (Tris-HCl, pH 7.6, 1 M NaCl, 20 mM imidazole, 20 mM β-mercaptoethanol, 50% glycerol). The His-tagged protein was eluted with 250 mM imidazole in buffer B and then dialyzed against 40 mM Tris-HCl buffer, pH 7.6, 100 mM KCl, 1 mM dithiothreitol (DTT), 50% glycerol using a PD-10 desalting column (GE Healthcare). Purified proteins were visualized by 12% SDS-PAGE followed by Coomassie staining. The protein concentrations were initially estimated by the Bradford methods, and then the purity was evaluated after SDS-PAGE using a Bio-Rad Experion system (IFR88 Transcriptomic facility). The absence of DnaK in purified fractions of DnaJ mutants was assayed by Western blot by using a DnaK-specific antiserum (laboratory collection of Genevaux) (data not shown).

In Vitro Excision Assay—Linear *att* sites were amplified by PCR with primer pairs attL-SpeI/attL-KpnI for *att*L and attR-XbaI/attR-IHF2 for *att*R and then purified using the QIAquick PCR purification kit protocol (Qiagen). Reaction mixtures (50 μl) included linear *att* DNA sites (32 nM) in buffer containing 27 mM Tris-HCl, pH 7.6, 35 mM KCl, 10 mM spermidine, 1 mM EDTA, 1 mg/ml^{-1} acetylated BSA, 15% glycerol. IHF (0.25 μM), IntS (0.8 μM), TorI (1.6 μM), and DnaJ (3 μM) were added as indicated in the figures legends. TorI and DnaJ were initially preincubated at 37 °C for 30 min, and then IntS, IHF, and linear *att*L and *att*R DNA were simultaneously added. The reactions were carried out in optimized conditions at 37 °C for 1 h at an IHF:IntS:TorI:DnaJ protein ratio of 1:3:6:12. Reaction products were purified (QIAquick kit, Qiagen) and mixed with SYBR Green I (0.01%) before separation in a 2.5% agarose gel. The abundance of *att*P formed during *in vitro* excision assays was quantified by real time PCR as described (12) on a Mastercycler Ep Realplex (Eppendorf) using the SYBR Premix Ex *Taq*™ kit (TaKaRa) according to the manufacturer's instructions.

In Vivo Excision Assay and Real Time PCR Analysis—Strains MC4100, *dnaJ*::Tn*10–42* (Tet^R), and *dnaJ259* were grown at 30 °C in LB medium until the A_{600} reached 0.1 unit, bicyclomycin (100 μg·ml^{-1}) was added, and the growth resumed for 3 h at 30 °C under agitation. Control cells were grown without bicyclomycin. Appropriate culture dilutions were plated onto LB medium. The proportion of *att*L site in a colony was estimated by Q-PCR on colonies using the primer pair attL-ter and attL-pro. In parallel, the genes *mglC*, *htpG*, and *gpt* were amplified by Q-PCR on the same colonies to evaluate the number of chromosomal copies using appropriate primer pairs (Table 1). Each colony was diluted in 20 μl of water, incubated for 10 min at 98 °C, and then transferred on ice. Q-PCRs were carried out as described above.

Electrophoretic Mobility Shift Assays (EMSAs)—EMSAs were carried out using purified proteins and fluorescently Cy5-la-

beled *att*L and p*nupG* DNA fragments that were PCR-amplified using MC4100 chromosomal DNA as a template with the primers pairs attL-pro/attL-ter-Cy5 and pnupG-L-Cy5/pnupG-R. DNA and purified proteins were mixed together at different concentrations (as indicated in the figure legends) in the presence of 4 mg·ml^{-1} BSA and 0.5 mg·ml^{-1} calf thymus DNA in buffer (40 mM Tris, pH 7.6, 50 mM KCl, 24% glycerol). Reactions were incubated for 30 min at room temperature. DNA-protein complexes were then separated using a 6% non-denaturing polyacrylamide gel (37:1 acrylamide:bisacrylamide ratio). A premigration step (1 h at 160 V) was carried out to reduce ionic charges, which may have destabilized the DNA-protein complex. Samples were then loaded and left to migrate at 90 V for 30 min and then at 160 V for an additional 2 h in 0.5× Tris borate-EDTA running buffer. The gel was scanned using an FLA5100 (Fuji) scanner using an excitation wavelength of 635 nm (800-V scanning intensity) and an emission wavelength of 665 nm. Data were analyzed using MultiGauge (version 2.3) software.

Luciferase Refolding Assay—Reactivation of firefly luciferase was performed essentially as described (30) with minor modifications. Briefly, luciferase (Sigma) at a concentration of 25 μM was denatured for 2 h at 22 °C in a solution containing 30 mM Tris-HCl, pH 7.6, 6 M guanidinium chloride, 5 mM DTT. The denatured luciferase was diluted to a final concentration of 0.125 μM into a reaction mixture (50-μl final volume) containing 100 mM MOPS, 500 mM KCl, 50 mM $MgCl_2$, 20 mM creatine phosphate, 0.1 mg·ml^{-1} creatine kinase, 5 mM ATP, 0.015% bovine serum albumin, 0.5 μM DnaK, 0.125 μM GrpE. All components were incubated on ice. Renaturation was initiated by adding either DnaJ or DnaJ mutants (0.125 μM each). The luciferase activity was measured at different time points after incubation at 22 °C by using 10 μl of the luciferase assay system from Promega (E1500) and a Berthold Centro LB960 luminometer. Average values of two independent experiments were plotted.

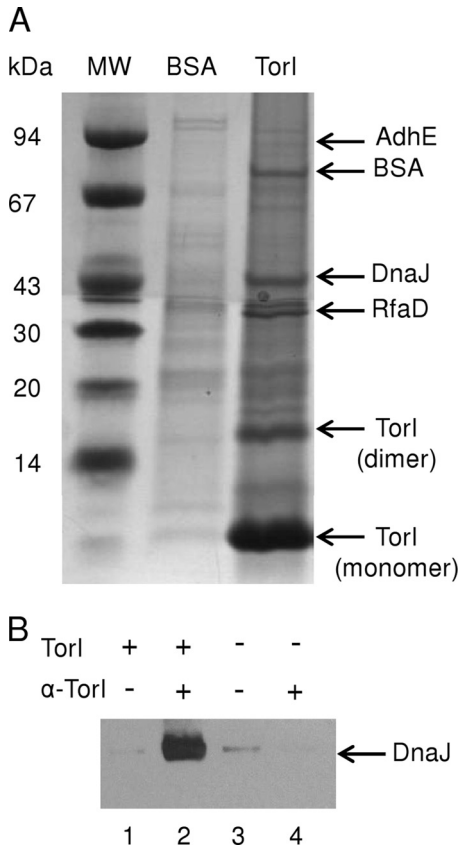

FIGURE 1. **DnaJ interacts with TorI RDF.** *A*, crude cell lysates of MG1655 cells grown exponentially were incubated with magnetic beads coated with TorI or BSA. After magnetic separation, bound proteins were eluted and separated by 12–16% Tricine SDS-PAGE. Proteins specifically bound to TorI beads in three independent experiments were analyzed by mass spectrometry. A typical gel is shown, and the main pulled down proteins are indicated by *arrows*. *B*, Δ^3 strain bearing plasmid encoding His-tagged wild-type DnaJ (pPGJ-His; *lanes 1–4*) was transformed with a TorI-encoding plasmid (pBTorI) (*lanes 1* and *2*). Cell lysates were subjected to immunoprecipitation with TorI antibody (*lanes 2* and *4*) or not (*lanes 1* and *3*), and samples were separated using Tricine SDS-PAGE, transferred to nitrocellulose, and probed with anti-DnaJ antibody.

RESULTS

DnaJ Interacts with TorI RDF—To identify new molecular partners of the TorI excisionase, a pulldown experiment was performed with a soluble fraction of *E. coli* cells grown in rich medium and harvested in exponential phase. The extract was incubated together with magnetic beads coated with TorI under native conditions; the beads were magnetically separated from the supernatant and washed extensively before elution of the bound proteins. A control experiment was carried out using beads coated with BSA and showed that all proteins eluted with TorI-coated beads were due to a specific interaction. The proteins from the elution fractions were separated using a 10–16% acrylamide Tricine-SDS gel and identified by MALDI mass spectrometry (Fig. 1*A*). The data shown are representative of three independent experiments. The most abundant protein found binding specifically to TorI is itself. This is a consequence of the propensity of TorI protein to oligomerize (11). Three other proteins proved to bind specifically to TorI under such conditions: the fused acetaldehyde-CoA dehydrogenase AdhE (96.1 kDa; P0A9Q7 UNIPROT), the cochaperone DnaJ (42 kDa; P08622), and the ADP-L-glycero-D-mannoheptose 6-epimerase RfaD (34.9 kDa; P67910). As DnaJ together with DnaK and GrpE has been shown to be involved in phage development as part of the replicative machinery (32, 33), the hypothesis that DnaJ and perhaps the complete DnaK/DnaJ/GrpE chaperone machine could specifically be involved in TorI-mediated excision was thus intriguing and deserved further attention. Therefore, we decided to first focus on DnaJ-TorI interaction. To confirm that TorI and DnaJ interaction was possible *in vivo* with non-purified TorI, an immunoprecipitation assay was performed using purified anti-TorI IgG. Both DnaJ-His_6 and TorI were co-expressed in the presence of 0.2% L-arabinose inducer in the Δ^3 strain. Note that under such conditions the cellular level of plasmid-encoded DnaJ is about 15-fold higher than endogenous DnaJ. The cell lysates were then incubated overnight with anti-TorI antibodies before magnetic separation of the bound proteins (Fig. 1*B*). As a result, DnaJ was efficiently pulled down only in the presence of the TorI-producing plasmid and when the cell lysate was incubated with anti-TorI specific antibodies (Fig. 1*B*, compare *lanes 1* and *2*). Note that a very low background level of DnaJ was found under each condition most likely due to nonspecific binding of DnaJ to the superparamagnetic particles or to protein A. Control experi-

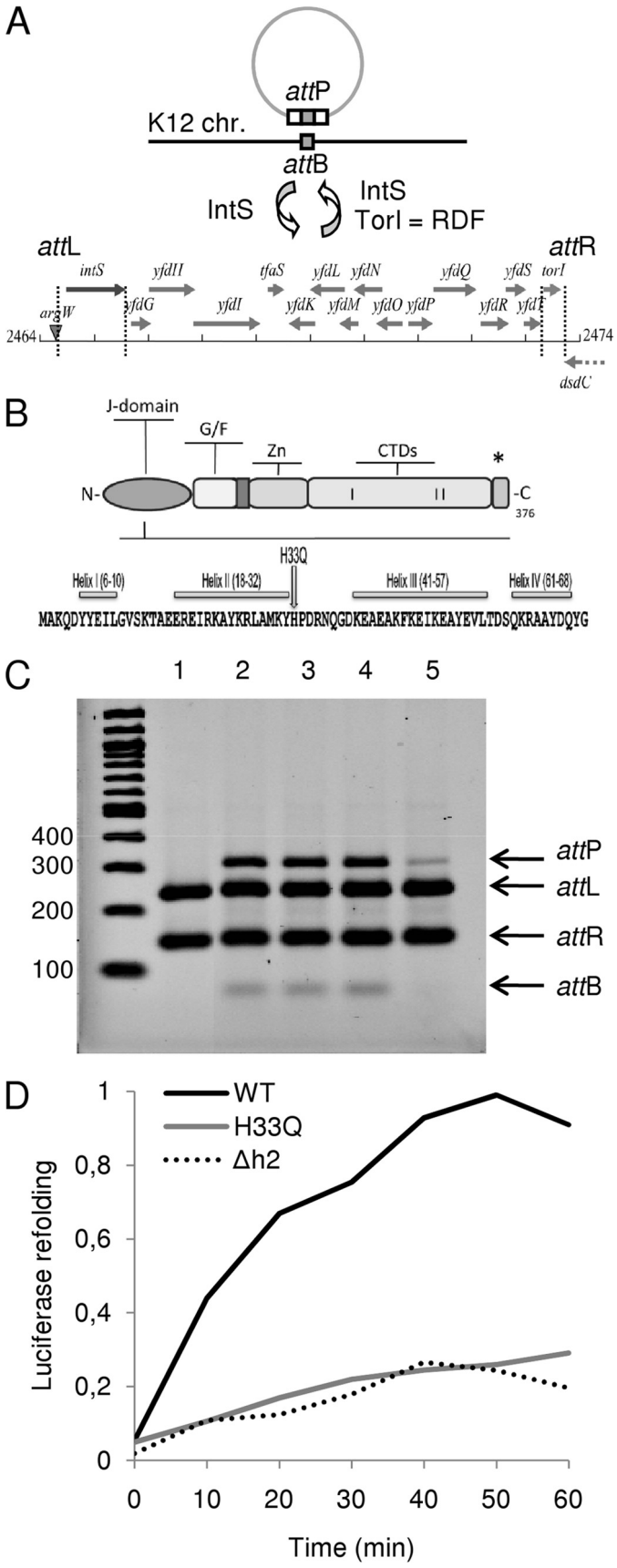

FIGURE 2. **DnaJ stimulates excision *in vitro* and does not require functional J-domain.** *A*, schematic representation of the site-specific recombination reaction. The KplE1 prophage is represented in the chromosomal context, and its 16 open reading frames are mentioned with *arrows* indicating the direction of transcription. *chr.*, chromosome. *B*, DnaJ domain representation. Domains of DnaJ are shown from the N to C terminus: J-domain, glycine-phenylalanine-rich (*G/F*), zinc finger domain (*Zn*), C-terminal domains I and II (*CTDs*), and * dimerization domain. The J-domain sequence and the four α-helices that compose this domain are indicated. The H33Q mutation (*dnaJ259*) is indicated by an *arrow*. *C*, *in vitro* excision assay in the presence of DnaJ wild type and variants. *In vitro* excision assays were performed with suboptimal concentrations of SSR proteins (0.5 μM TorI, 0.2 μM IntS, and 0.2 μM IHF). DnaJ wild type and mutants (3 μM) were added as follows: *lane 1*, no protein; *lane 2*, SSR + DnaJ; *lane 3*, SSR + DnaJΔh2; *lane 4*, SSR + DnaJH33Q; *lane 5*, SSR. After incubation for 1 h at 37 °C, reactions were loaded on a 2.5% agarose gel and quantified by real time PCR (see text). *D*, luciferase folding assay. DnaJ variant activity was assayed in an *in vitro* luciferase folding assay.

ments had shown that TorI and DnaJ antibodies did not cross-react (data not shown). Elution was performed under native conditions, and therefore some DnaJ-TorI complexes could be detected on the gel. Together, these results indicate a specific interaction between the TorI RDF protein and the cochaperone DnaJ.

DnaJ-TorI Interaction Is Functional—To pinpoint a possible role for DnaJ in KplE1 prophage site-specific recombination (Fig. 2*A*) in relation with the TorI excisionase, we included purified DnaJ protein in our *in vitro* excision assay (12). To detect a significant increase in excision activity, this experiment was performed under suboptimal protein concentrations (see "Experimental Procedures"). Remarkably, the presence of purified DnaJ in the reaction dramatically increased the excision efficiency (Fig. 2*C*, compare *lane 2* with *lane 5*). The reaction product *att*P was quantified by Q-PCR and was 30-fold more abundant in the presence of DnaJ compared with the control experiment performed in the absence of DnaJ (Fig. 2*C*, compare *lanes 2* and *5*), indicating that DnaJ increased the excision efficiency. These results demonstrate that the interaction between the TorI excisionase and the DnaJ chaperone is functional, thus revealing a critical role for DnaJ in KplE1 prophage excision.

As stated above, DnaJ generally acts in concert with its chaperone partner DnaK (Hsp70). As a *bona fide* cochaperone, it binds specific protein clients and delivers them to the DnaK chaperone, which then assists the folding reaction. However, our results suggested that DnaJ could efficiently perform in solo as a chaperone during prophage excision. To further prove that the effect of DnaJ on excision was related to its chaperone activity, we asked whether the DnaJ J-domain, which is absolutely required for its DnaK cochaperone function (34, 35), was also dispensable for site-specific recombination. Two different DnaJ mutants were thus assayed *in vitro*, *i.e.* DnaJH33Q with a His-33 to Gln amino acid substitution in the J-domain that abolishes all known DnaK cochaperone functions *in vivo* and *in vitro* (36) and DnaJΔh2 with a deletion of the second α-helix in the J-domain. As for DnaJH33Q, the DnaJΔh2 mutant lost its cochaperone activity (Fig. 2*D*). In contrast, both DnaJ mutants stimulated the *in vitro* excision in a similar manner to that of the DnaJ wild-type protein (Fig. 2*C*, compare *lanes 3* and *4* with *lane 2*). To make sure that DnaK was not co-purified with the mutant forms of DnaJ, we tested the DnaJ fractions by Western blot, which confirmed the absence of DnaK (data not shown). Taken together, these results indicate that DnaJ stimulates KplE1 excision *in vitro* independently of DnaK and that its J-domain is not involved in this process. However, at this stage, we cannot

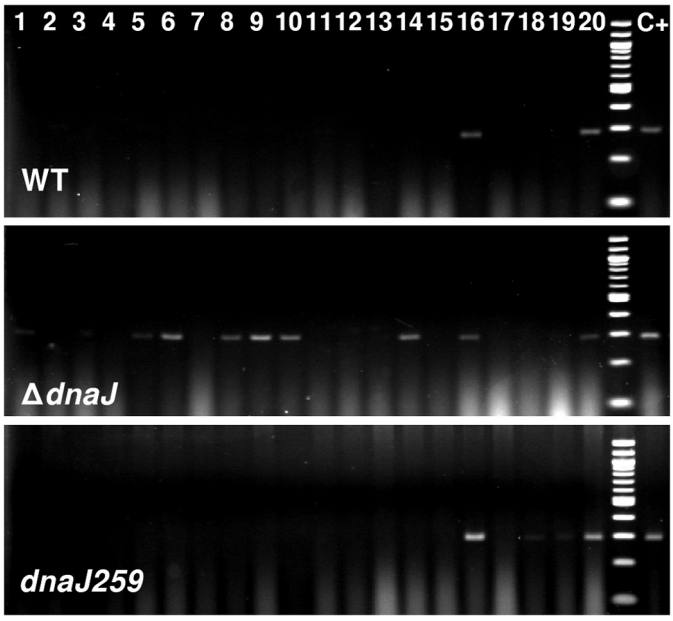

FIGURE 3. **DnaJ stimulates KplE1 excision *in vivo*.** Colony PCR was performed on wild-type, *dnaJ*::Tn*10*–*42*, and *dnaJ259* cells treated with bicyclomycin to induce KplE1 excision. Amplification of the *att*L recombination region is possible only when KplE1 is not excised. A total of 240 (WT), 180 (Δ*dnaJ*), and 100 (*dnaJ259*) colonies were assayed, and typical results are shown for 20 colonies (1–20). The control lane (*C*+) corresponds to the amplification of an untreated wild-type colony. Percentages of excision were calculated according to the Q-PCR results and were as follow: 98% (WT), 51% (Δ*dnaJ*), and 95% (*dnaJ259*).

exclude further involvement of DnaK in this process because we could not assay DnaK *in vitro*. Indeed, despite extensive trials, the experimental conditions for DnaK chaperone activity *in vitro* proved to be incompatible with the SSR reaction (see "Experimental Procedures"). In particular, the high KCl concentration required for DnaK function totally inhibited the recombination reaction.

KplE1 Excision Is Impaired in Absence of DnaJ in Vivo—KplE1 is a defective prophage that lacks both the lytic and the Δ repressor modules. As a result, KplE1 is not inducible by the SOS response. We have previously shown that the integrase gene, *intS*, is expressed in exponential growth phase and that TorI production from a multicopy plasmid is sufficient to promote KplE1 excision *in vivo* (10, 12, 18). In *E. coli*, a large proportion of prophage genes are negatively controlled by the Rho transcription terminator (37). Indeed, in the presence of a Rho-specific inhibitor (bicyclomycin), we found that the *torI* gene was transcribed at a level sufficient enough to promote *in vivo* excision because the integrase gene is constantly expressed at a level sufficient to allow excision.[4] *In vivo* excision assays were thus carried out in the presence of bicyclomycin in various genetic backgrounds and assayed by colony PCR and colony Q-PCR using specific primers for *att*L amplification. As shown in Fig. 3, the addition of 100 $\mu g \cdot ml^{-1}$ bicyclomycin to a wild-type cell culture led to a significant increase in KplE1 excision. The excision efficiency was quantified by Q-PCR, and only 2% of the cells contained an *att*L site. In contrast, in a *dnaJ*-null background, the excision efficiency dropped, and *att*L could be amplified in 50% of the cells, revealing at least a 20-fold decrease in *in vivo* excision. To investigate whether a functional interaction of DnaJ with DnaK was dispensable *in vivo*, we took advantage of the well characterized *dnaJ259* mutant allele, which encodes a DnaJ protein with the His-33 to Gln amino acid substitution. As described above, such DnaJH33Q mutant is unable to stimulate DnaK but retains all its known substrate binding properties. In this case, the *dnaJ259* allele (DnaJH33Q) should support excision as well as the wild-type allele, although it does not stimulate DnaK activity. Indeed, in such a genetic background, excision was as efficient as in the presence of wild-type DnaJ (Fig. 3). These data demonstrate that DnaJ is capable of stimulating KplE1 excision *in vivo* independently of DnaK, a result that is in full agreement with the data obtained *in vitro*.

DnaJ Stimulates TorI DNA Binding Activity on attL—The TorI protein is a bifunctional protein that has protein and DNA binding activities (10, 11, 15). Because TorI was shown to bind DnaJ, an attractive hypothesis was that DnaJ was recruited to the recombination region by TorI. Accordingly, EMSA was used to characterize the possible role of DnaJ in TorI binding to *att*L DNA. All reaction conditions were carried out in the presence of calf thymus DNA and BSA to reduce the occurrence of nonspecific DNA-protein interactions and Cy5-labeled DNA. In these conditions, there was no direct interaction between *att*L and DnaJ at different DnaJ protein concentrations (5 and 10 μM) as there was no change in the distance of migration of *att*L (Fig. 4*A*, *lanes 14* and *15* compared with *lane 13*). As expected, low concentrations of TorI (0.5 μM) were insufficient to result in a significant binding of *att*L (Fig. 4*A*, *lane 10*). However, the effect of DnaJ was clearly marked at 1 μM TorI (Fig. 4*A*, *lane 7*): remarkably, in this case, the addition of DnaJ triggered TorI binding to *att*L, which resulted in a shift in the migration distance of the target DNA (Fig. 4*A*, *lanes 8* and *9*). Similar results were found with higher concentrations of TorI where TorI was able to bind and shift more *att*L in the presence of DnaJ (Fig. 4*A*, *lanes 5* and *6*). This increased shift of DNA was still evident although subtle when high concentrations of TorI were used (Fig. 4*A*, *lanes 2* and *3* compared with *lane 1*). Additional control experiments showed that when using a nonspecific DNA probe, such as the p*nupG* promoter, which is not bound by TorI, DnaJ did not provoke TorI-DNA binding (Fig. 4*A*, *lanes 16*–*21*). This result demonstrates that DnaJ specifically stimulates TorI binding to its DNA target and is in full agreement with the increased excisive recombination activity found in the *in vitro* recombination assays (Fig. 2*C*). Furthermore, no additional shift of the *att*L target DNA could be observed in the presence of DnaJ compared with the shift observed in the presence of TorI alone, and no DnaJ could be detected at the level of the TorI-*att*L complex by Western blot using a DnaJ antiserum because DnaJ barely entered the gel under native conditions (Fig. 4*B*). This suggests that DnaJ is not part of the final TorI-*att*L complex and rather has a transient role in agreement with a *bona fide* chaperone activity.

DISCUSSION

Viruses are reliant on host cell machineries for productive infection, and molecular chaperones have long been described as important elements of viral infection (for reviews, see Refs.

[4] R. Menouni and M. Ansaldi, unpublished results.

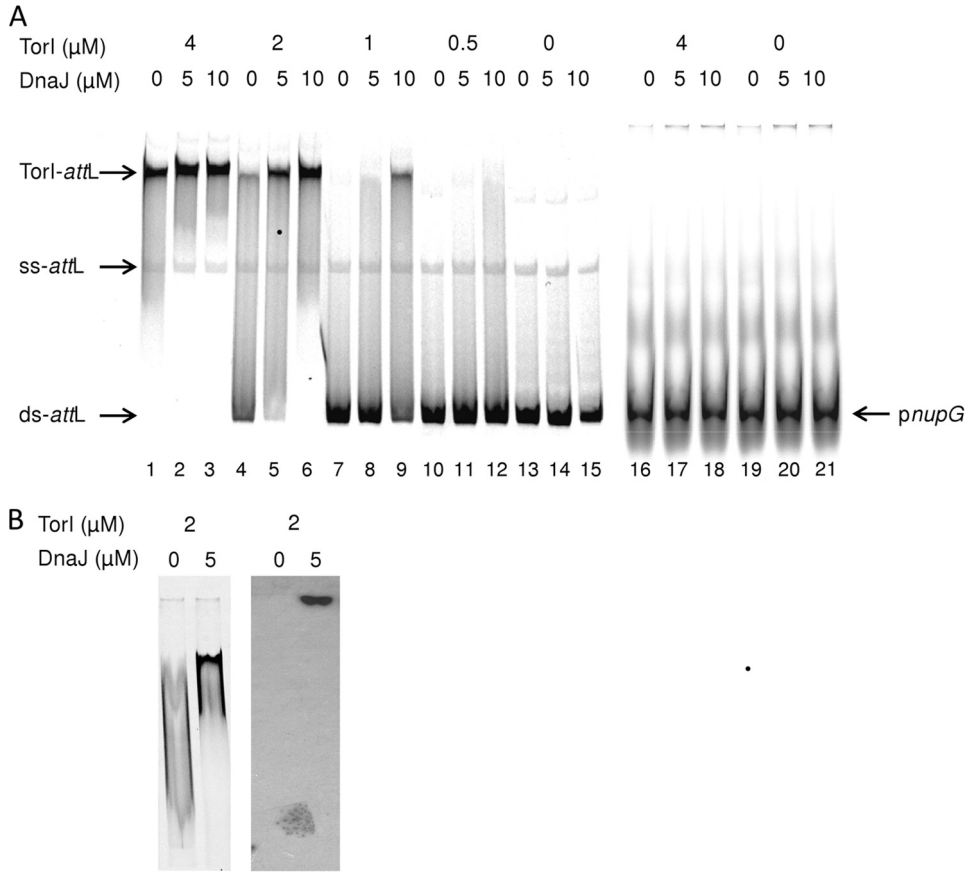

FIGURE 4. **DnaJ enhances TorI DNA binding activity *in vitro*.** *A*, EMSA experiments were performed in the presence of various TorI and DnaJ protein concentrations as described under "Experimental Procedures." *Arrows* indicate the different forms of Cy5-labeled DNA: *ds-attL*, unbound double-stranded DNA; *ss-attL*, single-stranded unbound *att*L DNA; *TorI-attL*, double-stranded TorI-bound DNA; and p*nupG*. Note that the presence of single-stranded unbound *att*L DNA is an artifact form that does not shift in the presence of any of the proteins. *B*, EMSA experiments were performed in the presence of 1 mM TorI and 5–10 mM DnaJ, the gel was then transferred, and the blot was immunoassayed with a DnaJ antibody.

38 and 39). As an example, Hsp70 proteins are involved in multiple steps of virus development, such as cell entry, nuclear import for eukaryotic viruses, replication, and assembly. It is interesting to note that some viruses, including T4 phage and simian virus 40 (SV40), encode their own chaperones or cochaperones that are involved in DNA replication and/or virion assembly (40–42).

The *E. coli* chaperonins (GroEL/GroES) and the DnaJ/DnaJ/GrpE chaperone machine have been identified through a genetic screen that focused on λ phage development (22, 26, 43). It was initially discovered that the DnaK/DnaJ/GrpE machine plays a key role in λ phage replication through disassembly of the λO-λP-DnaB complex at oriλ. This results in the release of λP and the initiation of DNA replication by the functional λO-DnaB complex (44, 45). However, no roles have ever been described for these chaperones in lysogeny escape. Thus, the finding that the stress chaperone DnaJ is involved in prophage excision constitutes a new link between an early step of the switch from lysogeny to lytic development and the heat shock response.

The newly identified interaction between TorI and DnaJ (Fig. 1) suggested that such an interaction could have an impact on the excisive recombination of the KplE1 prophage. Indeed, when added to the *in vitro* excision assay, DnaJ provoked a dramatic increase in recombination efficiency. Remarkably, such stimulatory effect of DnaJ did not require the presence of either its DnaK and GrpE partners or a functional J-domain (Fig. 2). This effect was further supported *in vivo* because in a *dnaJ*-null background the efficiency of the excisive recombination was significantly impaired when compared with both wild-type and *dnaJ259* strains (Fig. 4). Taken together, these data demonstrate that solitary DnaJ stress chaperone is capable of stimulating prophage excision and is thus involved in a prereplicative step of lytic development.

All the known DnaJ activities *in vivo* are linked to its DnaK cochaperone functions. However, DnaJ can bind substrates *in vitro* and protect them from aggregation independently of DnaK. Such chaperone function of DnaJ is carried out by its central zinc-binding domain, its C-terminal domains, and most likely its glycine-phenylalanine-rich region (46) and is thus unrelated to a functional J-domain (47–49). Although we cannot firmly exclude an involvement of DnaK, our results strongly suggest that stimulation of TorI-mediated excision by DnaJ solely relies on such chaperone functions. Indeed, the *dnaJ259* allele, which is thermosensitive and does not support λ phage replication (50), behaves *in vivo* like a wild-type *dnaJ* (Fig. 4).

What is remarkable in TorI-DnaJ interaction is that upon binding to its specific DNA target TorI seems to be efficiently released from DnaJ without the need for downstream DnaK and GrpE, thus further supporting a DnaK-independent func-

tion. Such an observation is in sharp contrast with the role performed by DnaJ during protein export where presecretory substrate release from DnaJ to the degradation machinery required both DnaK and GrpE (51). As a *bona fide* chaperone, DnaJ plays a major role in mini-F plasmid replication by stimulating RepE binding to the origin *in vitro* (47). Therefore, the TorI and RepE proteins constitute folded substrates for DnaJ, and such interactions modify the DNA binding ability of the two substrates. Although RepE and TorI are both DNA-binding proteins (10, 52, 53), the overall shapes of the proteins do not provide sufficient similarity to propose a particular structural motif that could be involved in DnaJ binding. In the case of RepE, DnaK and GrpE are also involved in this process because the mini-F plasmid does not replicate in any individual mutant of the DnaK/DnaJ/GrpE machine (54). Such a scenario could also be applied to the original KplE1 phage genome, which integrated at the *argW* tRNA site. However, because KplE1 became non-replicative, this dependence could no longer be observed, and excisive recombination likely relies solely on DnaJ.

We show that DnaJ enhances the binding of TorI to its specific DNA substrate. TorI binds to five distinct sites on the *att*L recombination region of the KplE1 prophage in a highly cooperative manner (11). However, our data unambiguously demonstrate that the affinity of TorI for the *att*L substrate strongly increases in the presence of DnaJ, which does not bind itself to this DNA substrate. The *E. coli* J-domain-containing proteins, such as DnaJ, have been described as able to bind DNA (55); however, using the *att*L and p*nupG* substrates and stringent conditions (competitor DNA in 100-fold excess), we did not observe any DnaJ binding to DNA (Fig. 3). Moreover, in the presence of both TorI and DnaJ, the nucleoprotein complex formed with *att*L migrated similarly to that in the presence of TorI alone, suggesting that DnaJ is not present in the final complex. An attractive hypothesis is that DnaJ remodels TorI in a conformation that increases its affinity to its DNA target, and upon binding, the chaperone would subsequently be released from TorI. We can also predict that other recombination systems, in particular those of the infectious phages HK620 and Sf6 that contain highly similar recombination modules (12), will be enhanced by DnaJ.

With respect to temperate phage development, it is tempting to link stress induction of lysogeny escape to chaperone-mediated excisive recombination. Indeed, heat shock has been shown to induce the λ prophage through a slightly different regulatory path than the DNA damage pathway (56). However, to date, no apparent link has been identified between excisive recombination and the heat shock response, although excision of the prophage genome is a crucial step following the decision to switch from lysogeny to the lytic mode.

Acknowledgments—We thank S. Lignon from the Institut de Microbiologie de la Méditerranée (IMM) Proteomic Platform (CNRS, Marseille, France) for protein identification, Y. Denis from the IMM Transcriptomic facility (CNRS, Marseille, France) for the use of Experion equipment and Q-PCR advice, and L. Alossuo and A.-M. Cirinesi for technical assistance. We thank V. Méjean and G. Panis for stimulating discussions and T. Mignot for critical reading of the manuscript.

REFERENCES

1. Brüssow, H., Canchaya, C., and Hardt, W. D. (2004) *Microbiol. Mol. Biol. Rev.* **68,** 560–602
2. Campbell, A. M. (1996) in *Escherichia coli and Salmonella: Cellular and Molecular Biology* (Neidhardt, F. C., ed) pp. 2041–2046, ASM Press, Washington, D. C.
3. Nash, H. (1996) in *Escherichia coli and Salmonella: Cellular and Molecular Biology* (Neidhardt, F. C., ed) pp. 2363–2376, ASM Press, Washington, D. C.
4. Oppenheim, A. B., Kobiler, O., Stavans, J., Court D. L., and Adhya, S. (2005) *Annu. Rev. Genet.* **39,** 409–429
5. Gottesman, S., and Abremski, K. (1980) *J. Mol. Biol.* **138,** 503–512
6. Abremski, K., and Gottesman, S. (1982) *J. Biol. Chem.* **257,** 9658–9662
7. Lewis, J. A., and Hatfull, G. F. (2001) *Nucleic Acids Res.* **29,** 2205–2216
8. Mumm, J. P., Landy, A., and Gelles, J. (2006) *EMBO J.* **25,** 4586–4595
9. Casjens, S. (2003) *Mol. Microbiol.* **49,** 277–300
10. Elantak, L., Ansaldi, M., Guerlesquin, F., Méjean, V., and Morelli, X. (2005) *J. Biol. Chem.* **280,** 36802–36808
11. Panis, G., Duverger, Y., Champ, S., and Ansaldi, M. (2010) *Virology* **404,** 41–50
12. Panis, G., Méjean, V., and Ansaldi, M. (2007) *J. Biol. Chem.* **282,** 21798–21809
13. Clark, A. J., Inwood, W., Cloutier, T., and Dhillon, T. S. (2001) *J. Mol. Biol.* **311,** 657–679
14. Casjens, S., Winn-Stapley, D. A., Gilcrease, E. B., Morona, R., Kühlewein, C., Chua, J. E., Manning, P. A., Inwood, W., and Clark, A. J. (2004) *J. Mol. Biol.* **339,** 379–394
15. Ansaldi, M., Théraulaz, L., and Méjean, V. (2004) *Proc. Natl. Acad. Sci. U.S.A.* **101,** 9423–9428
16. Sam, M. D., Papagiannis, C. V., Connolly, K. M., Corselli, L., Iwahara, J., Lee, J., Phillips, M., Wojciak, J. M., Johnson, R. C., and Clubb, R. T. (2002) *J. Mol. Biol.* **324,** 791–805
17. Abbani, M., Iwahara, M., and Clubb, R. T. (2005) *J. Mol. Biol.* **347,** 11–25
18. Panis, G., Duverger, Y., Courvoisier-Dezord, E., Champ, S., Talla, E., and Ansaldi, M. (2010) *PLoS Genet.* **6,** e1001149
19. Bukau, B., Weissman, J., and Horwich, A. (2006) *Cell* **125,** 443–451
20. Hartl, F. U., and Hayer-Hartl, M. (2009) *Nat. Struct. Mol. Biol.* **16,** 574–581
21. Mayer, M. P. (2005) *Rev. Physiol. Biochem. Pharmacol.* **153,** 1–46
22. Georgopoulos, C. P. (1977) *Mol. Gen. Genet.* **151,** 35–39
23. Friedman, D. I., Olson, E. R., Georgopoulos, C., Tilly, K., Herskowitz, I., and Banuett, F. (1984) *Microbiol. Rev.* **48,** 299–325
24. LeBowitz, J. H., Zylicz, M., Georgopoulos, C., and McMacken, R. (1985) *Proc. Natl. Acad. Sci. U.S.A.* **82,** 3988–3992
25. Gaitanaris, G. A., Vysokanov, A., Hung, S. C., Gottesman, M. E., and Gragerov, A. (1994) *Mol. Microbiol.* **14,** 861–869
26. Georgopoulos, C. (2006) *Genetics* **174,** 1699–1707
27. Genevaux, P., Georgopoulos, C., and Kelley, W. L. (2007) *Mol. Microbiol.* **66,** 840–857
28. Zylicz, M., Liberek, K., Wawrzynow, A., and Georgopoulos, C. (1998) *Proc. Natl. Acad. Sci. U.S.A.* **95,** 15259–15263
29. Zylicz, M. (1993) *Philos. Trans. R. Soc. Lond. B Biol. Sci.* **339,** 271–278
30. Cajo, G. C., Horne, B. E., Kelley, W. L., Schwager, F., Georgopoulos, C., and Genevaux, P. (2006) *J. Biol. Chem.* **281,** 12436–12444
31. Ansaldi, M., Lepelletier, M., and Méjean, V. (1996) *Anal. Biochem.* **234,** 110–111
32. Liberek, K., Osipiuk, J., Zylicz, M., Ang, D., Skorko, J., and Georgopoulos, C. (1990) *J. Biol. Chem.* **265,** 3022–3029
33. Osipiuk, J., Georgopoulos, C., and Zylicz, M. (1993) *J. Biol. Chem.* **268,** 4821–4827
34. Suh, W. C., Burkholder, W. F., Lu, C. Z., Zhao, X., Gottesman, M. E., and Gross, C. A. (1998) *Proc. Natl. Acad. Sci. U.S.A.* **95,** 15223–15228
35. Genevaux, P., Schwager, F., Georgopoulos, C., and Kelley, W. L. (2002) *Genetics* **162,** 1045–1053
36. Wall, D., Zylicz, M., and Georgopoulos, C. (1994) *J. Biol. Chem.* **269,** 5446–5451
37. Cardinale, C. J., Washburn, R. S., Tadigotla, V. R., Brown, L. M., Gottes-

man, M. E., and Nudler, E. (2008) *Science* **320,** 935–938
38. Sullivan, C. S., and Pipas, J. M. (2001) *Virology* **287,** 1–8
39. Xiao, A., Wong, J., and Luo, H. (2010) *Arch. Virol.* **155,** 1021–1031
40. van der Vies, S. M., Gatenby, A. A., and Georgopoulos, C. (1994) *Nature* **368,** 654–656
41. Srinivasan, A., McClellan, A. J., Vartikar, J., Marks, I., Cantalupo, P., Li, Y., Whyte, P., Rundell, K., Brodsky, J. L., and Pipas, J. M. (1997) *Mol. Cell. Biol.* **17,** 4761–4773
42. Genevaux, P., Lang, F., Schwager, F., Vartikar, J. V., Rundell, K., Pipas, J. M., Georgopoulos, C., and Kelley, W. L. (2003) *J. Virol.* **77,** 10706–10713
43. Maynard, N. D., Birch, E. W., Sanghvi, J. C., Chen, L., Gutschow, M. V., and Covert, M. W. (2010) *PLoS Genet.* **6,** e1001017
44. Wickner, S. H. (1979) *Cold Spring Harb. Symp. Quant. Biol.* **43,** 303–310
45. Zylicz, M., Ang, D., Liberek, K., and Georgopoulos, C. (1989) *EMBO J.* **8,** 1601–1608
46. Perales-Calvo, J., Muga, A., and Moro, F. (2010) *J. Biol. Chem.* **285,** 34231–34239
47. Kawasaki, Y., Wada, C., and Yura, T. (1992) *J. Biol. Chem.* **267,** 11520–11524
48. Szabo, A., Korszun, R., Hartl, F. U., and Flanagan, J. (1996) *EMBO J.* **15,** 408–417
49. Shi, Y. Y., Tang, W., Hao, S. F., and Wang, C. C. (2005) *Biochemistry* **44,** 1683–1689
50. Sell, S. M., Eisen, C., Ang, D., Zylicz, M., and Georgopoulos, C. (1990) *J. Bacteriol.* **172,** 4827–4835
51. Sakr, S., Cirinesi, A. M., Ullers, R. S., Schwager, F., Georgopoulos, C., and Genevaux, P. (2010) *J. Biol. Chem.* **285,** 23506–23514
52. Huang, W., Yuan, C., Ansaldi, M., Morelli, X., Meehan, E. J., Chen, L. Q., and Huang, M. (2007) *Chin. J. Struct. Chem.* **26,** 594–598
53. Nakamura, A., Wada, C., and Miki, K. (2007) *Proc. Natl. Acad. Sci. U.S.A.* **104,** 18484–18489
54. Kawasaki, Y., Wada, C., and Yura, T. (1990) *Mol. Gen. Genet.* **220,** 277–282
55. Gur, E., Katz, C., and Ron, E. Z. (2005) *FEBS Lett.* **579,** 1935–1939
56. Rokney, A., Kobiler, O., Amir, A., Court DL, Stavans, J., Adhya, S., and Oppenheim, A. B. (2008) *Mol. Microbiol.* **68,** 29–36
57. Genevaux, P., Schwager, F., Georgopoulos, C., and Kelley, W. L. (2001) *J. Bacteriol.* **183,** 5747–5750